Eur. Phys. J. D (2023) 77:6
https://doi.org/10.1140/epjd/s10053-022-00589-y

THE EUROPEAN PHYSICAL JOURNAL D

Regular Article – Atomic and Molecular Collisions

Relative importance of the electron continuum intermediate state in single-electron capture into any state of fast protons from helium-like atomic systems

Danilo Delibašić[a]

Department of Physics, Faculty of Sciences and Mathematics, Višegradska 33, Niš 18000, Serbia

Received 31 October 2022 / Accepted 19 December 2022 / Published online 4 January 2023

Abstract. Single-electron capture by fast protons from helium-like atomic targets is investigated at intermediate and high impact energies. The main purpose of the present study is a comprehensive analysis of the relative importance of the electron continuum intermediate state (ionization continua), with respect to direct transfer. To achieve this goal, first- and second-order theories are employed, and their results are thoroughly compared. The prior form of the boundary-corrected continuum intermediate state method (BCIS) is utilized, in both its three-body and four-body formulation, in addition to the four-body boundary-corrected first-Born approximation (CB1-4B), in both its prior and post form. BCIS methods belong to the class of second-order theories, while CB1 methods belong to the class of first-order theories. Relative importance of ionization continua is examined in the example of single-electron capture in collisions of fast protons with ground-state atomic helium. Both differential and total cross sections are analyzed, for single-electron capture into any final state of the projectile. The presented cross sections, aside from their fundamental importance, are relevant in various interdisciplinary applications, such as in astrophysics, thermonuclear fusion and plasma physics, and medical physics.

1 Introduction

The phenomenon of single-electron capture, as well as charge exchange in general, has attracted significant scientific interest almost since the dawn of quantum mechanics. The first steps were undertaken in the pioneering work of Oppenheimer [1] and Brinkman and Kramers [2]. Charge exchange has since been the subject of numerous investigations, both theoretical and experimental [3–24]. Cross sections for various charge-exchange processes cannot be calculated analytically, so different approximation methods have been developed. These can be divided into perturbative [3–7,25–39] and non-perturbative [40–48]. Generally speaking, perturbative approaches are adequate for describing high-energy collisions, while non-perturbative are more appropriate at low impact energy values. The reference value for defining "low" and "high" is the energy of projectile moving with the speed of electron participating in the charge-exchange process. This energy of course varies for different projectiles and targets, but, in the described framework, the energy limit is usually taken to be around 20 keV. Energies below this will be considered as low, while up to about an order of magnitude larger (more precisely, up to 400 keV) will be considered as intermediate. Energies above 400 keV will be considered as high. In this work, we are interested in high-energy collisions, so various perturbative approaches will be utilized.

The main goal of the present study is a comprehensive analysis of the relative importance of the electron continuum intermediate state (ionization continua) with respect to direct transfer. The study will be performed in the example of single-electron capture in collisions of high-energy protons with ground-state atomic helium. The results will include both differential and total, as well as state-resolved and state-summed cross sections. Wherever they are available, the obtained theoretical results will be compared with the measurements, in order to truly assess the importance of the influence of continuum intermediate states upon the values of cross sections. The theoretical results include different first- and second-order theories. More precisely, the prior [29] and post [30,31] forms of the four-body boundary-corrected first-Born approximation (CB1-4B) method, as well as the prior form of the boundary-corrected continuum intermediate state method (BCIS) in its three-body (BCIS-3B) [32] and four-body (BCIS-4B) [33] formulation will be utilized. CB1-4B, both prior and post, are first-order, while BCIS-3B and BCIS-4B are second-order methods. The BCIS-3B method is effectively employed to this

[a] e-mail: danilo.delibasic@pmf.edu.rs (corresponding author)

fundamentally four-body problem. The reason for inclusion of the BCIS-3B results is that no state-resolved cross sections are available in the BCIS-4B method, while they are in the BCIS-3B. The reason for inclusion of the CB1-4B post form results is to determine whether any possible discrepancy between the prior form BCIS and CB1-4B methods could be ascribed to the use of non-exact helium ground-state wave function. In addition, while BCIS-3B is used as an effective approach, the hydrogenic wavefunction it employs is exact (in contrast with the helium ground-state wavefunction). All of these methods should provide just about enough data to properly determine the importance of ionization continua.

The present study is significant from a fundamental perspective, regarding the determination of importance of ionization continua in single-electron capture. In addition to this, the obtained cross sections are relevant in various interdisciplinary applications as well. For instance, these cross sections are needed in various astrophysical scenarios [49], thermonuclear fusion and plasma physics [50–53], as well as medical physics [8,54–61].

Atomic units will be used throughout unless otherwise stated.

2 Theory

In this work, we are interested in the following collision:

$$p + \mathrm{He}(1s^2) \longrightarrow \mathrm{H}(nlm) + \mathrm{He}^+(1s)\,, \tag{1}$$

i.e., single-electron capture by fast protons from the ground-state atomic helium into arbitrary final states (nlm is the usual triplet of quantum numbers). No excitation of the non-captured electron is considered, i.e., the target final state is a hydrogen-like ground state.

The application of CB1-4B and BCIS-4B methods to the collision given by Eq. (1) is straightforward, in the sense that we need to calculate the transition amplitude for the following general collision type:

$$\begin{aligned} &Z_\mathrm{P} + (Z_\mathrm{T}; e_1, e_2)_{1s^2} \\ &\longrightarrow (Z_\mathrm{P}; e_1)_{nlm} + (Z_\mathrm{T}; e_2)_{1s}\,, \end{aligned} \tag{2}$$

where Z_P and Z_T are the projectile (P) and target (T) nuclear charges, and e_1 and e_2 are the two electrons (initially bound to the target nuclei). The application of the BCIS-3B method, however, obviously requires some additional assumptions, to enable us to apply a three-body method to a fundamentally four-body problem. To this end, we adopt the independent-particle model and the frozen-core approximation [23], since no excitation of the remaining non-captured electron is considered. In this framework, we can treat the original target $(Z_\mathrm{T}; e_1, e_2)_{1s^2}$ as a hydrogen-like one $(Z_\mathrm{T}^\mathrm{eff}; e)_{1s}$. In other words, we explicitly consider only the *active* electron (the one that will be captured), while the remaining *passive* one influences the whole process of single-electron capture only through a shielding of the original target nuclei (hence the use of $Z_\mathrm{T}^\mathrm{eff}$ instead of Z_T). In light of these considerations, we can treat the original four-body problem (2) as an effectively three-body one:

$$Z_\mathrm{P} + (Z_\mathrm{T}^\mathrm{eff}; e)_{1s} \longrightarrow (Z_\mathrm{P}; e)_{nlm} + Z_\mathrm{T}^\mathrm{eff}\,, \tag{3}$$

thereby enabling a straightforward application of the three-body BCIS method.

The transition amplitude for the CB1-4B case, in its prior and post form, respectively, can be written as:

$$T_{if}^{CB1-} = \langle \Phi_f^- | V_i^c | \Phi_i^+ \rangle\,, \tag{4}$$

$$T_{if}^{CB1+} = \langle \Phi_f^- | V_f^c | \Phi_i^+ \rangle\,, \tag{5}$$

while the prior BCIS-3B and BCIS-4B transition amplitude takes the following form:

$$T_{if}^{BCIS-} = \langle \chi_f^- | V_i^c | \Phi_i^+ \rangle\,. \tag{6}$$

The wavefunctions in the entrance channel are denoted by Φ_i^+ in both cases (CB1 and BCIS), while in the exit channel they are denoted by Φ_f^- and χ_f^- in the CB1 and BCIS cases, respectively. The correct perturbation potential in the entrance channel is denoted by V_i^c, while in the exit channel it is denoted by V_f^c. The perturbation potentials V_i^c and V_f^c in the 3B and 4B cases are given by the following equations:

$$(V_i^c)^{3B} = \frac{Z_\mathrm{P} Z_\mathrm{T}}{R} - \frac{Z_\mathrm{P}(Z_\mathrm{T}-1)}{r_i} - \frac{Z_\mathrm{P}}{s}\,, \tag{7}$$

$$\begin{aligned} (V_i^c)^{4B} = &\frac{Z_\mathrm{P} Z_\mathrm{T}}{R} - \frac{Z_\mathrm{P}(Z_\mathrm{T}-2)}{r_i} \\ &- \frac{Z_\mathrm{P}}{s_1} - \frac{Z_\mathrm{P}}{s_2}\,, \end{aligned} \tag{8}$$

$$\begin{aligned} (V_f^c)^{4B} = &\frac{Z_\mathrm{P} Z_\mathrm{T}}{R} - \frac{(Z_\mathrm{P}-1)(Z_\mathrm{T}-1)}{r_f} \\ &- \frac{Z_\mathrm{T}}{x_1} - \frac{Z_\mathrm{P}}{s_2} + \frac{1}{r_{12}}\,, \end{aligned} \tag{9}$$

where $\vec{R}$ is the relative position vector between the projectile and target and $\vec{r}_i$ is the relative position vector between the center of mass of the projectile and target in the entrance channel, while $\vec{r}_f$ is the relative position vector between the center of mass of the target remainder and projectile in the exit channel. In the 3B case, $\vec{s}$ is the relative position vector between the electron e and the projectile nucleus, while in the 4B case, $\vec{s}_1$ and $\vec{s}_2$ are the relative position vectors between the electrons e_1 and e_2, respectively, and the projectile nucleus. In Eq. (9), $\vec{x}_1$ is the relative position vector between electron e_1 and the target nucleus. Finally, $\vec{r}_{12}$ is the relative position vector of electron e_1 with respect to electron e_2 (4B case). The reason for omission of the equation for BCIS post form transition amplitude

T_{if}^{BCIS+} (and the corresponding $(V_f^c)^{3B}$ in the BCIS-3B case) is that it is not considered in the present work.

As we can see from Eqs. (4) and (5), the prior and post forms of CB1-4B methods differ only in the perturbation potentials, while the wavefunctions in entrance and exit channels are the same, and, respectively, given by:

$$\begin{aligned}(\Phi_i^+)^{4B} &= \varphi_i(\vec{x}_1,\vec{x}_2)\\ &\quad\times e^{i\vec{k}_i\cdot\vec{r}_i+i\nu_i\ln(k_ir_i-\vec{k}_i\cdot\vec{r}_i)}\,, \qquad (10)\\ (\Phi_f^-)^{4B} &= \varphi_{\rm P}(\vec{s}_1)\varphi_{\rm T}(\vec{x}_2)\\ &\quad\times e^{-i\vec{k}_f\cdot\vec{r}_f-i\nu_f\ln(k_fr_f-\vec{k}_f\cdot\vec{r}_f)}\,, \qquad (11)\end{aligned}$$

with $\nu_i=\frac{Z_{\rm P}(Z_{\rm T}-2)}{v}$ and $\nu_f=\frac{(Z_{\rm P}-1)(Z_{\rm T}-1)}{v}$. Wavefunction $\varphi_i(\vec{x}_1,\vec{x}_2)$ is the initial helium-like ground-state wavefunction. In the present work, we utilized both the two-parameter wavefunction of Silverman et al. [62], as well as the four-parameter wavefunction of Löwdin [63]. The obtained results when using these two different wavefunctions are almost indistinguishable. In addition, $\varphi_{\rm P}(\vec{s}_1)\equiv\varphi_{nlm}(\vec{s}_1)$ and $\varphi_{\rm T}(\vec{x}_2)\equiv\varphi_{100}(\vec{x}_2)$ are the final projectile (arbitrary) and target (ground-state) hydrogen-like wavefunctions.

The prior forms of the BCIS methods share the wavefunction in the entrance channel and the perturbation potential with the corresponding CB1 methods (Eqs. (4) and (6)), while the only difference is in the exit channel wavefunction. The entrance channel wavefunction of the BCIS-3B method is given by:

$$(\Phi_i^+)^{3B}=\varphi_i(\vec{x})e^{i\vec{k}_i\cdot\vec{r}_i+i\nu_i\ln(k_ir_i-\vec{k}_i\cdot\vec{r}_i)}\,, \qquad (12)$$

with $\nu_i=\frac{Z_{\rm P}(Z_{\rm T}-1)}{v}$, while $\varphi_i(\vec{x})\equiv\varphi_{100}(\vec{x})$ is the initial hydrogen-like ground-state wavefunction. In the exit channel, the 3B and 4B wavefunctions are, respectively, given by:

$$\begin{aligned}(\chi_f^-)^{3B} &= \varphi_{\rm P}(\vec{s})e^{-i\vec{k}_f\cdot\vec{r}_f-i\nu\ln(k_fr_f-\vec{k}_f\cdot\vec{r}_f)}\\ &\quad\times N^-(\nu_{\rm T})\\ &\quad\times{}_1F_1(-i\nu_{\rm T},1,-ivx-i\vec{v}\cdot\vec{x})\,, \qquad (13)\\ (\chi_f^-)^{4B} &= \varphi_{\rm P}(\vec{s}_1)\varphi_{\rm T}(\vec{x}_2)e^{-i\vec{k}_f\cdot\vec{r}_f-i\nu'\ln(k_fr_f-\vec{k}_f\cdot\vec{r}_f)}\\ &\quad\times N^-(\nu'_{\rm T})\\ &\quad\times{}_1F_1(-i\nu'_{\rm T},1,-ivx_1-i\vec{v}\cdot\vec{x}_1)\,, \qquad (14)\end{aligned}$$

with $\nu=\frac{Z_{\rm P}Z_{\rm T}}{v}$, $\nu_{\rm T}=\frac{Z_{\rm T}}{v}$, $\nu'=\frac{Z_{\rm P}(Z_{\rm T}-1)}{v}$ and $\nu'_{\rm T}=\frac{Z_{\rm T}-1}{v}$. Wavefunction $\varphi_{\rm P}(\vec{s})\equiv\varphi_{nlm}(\vec{s})$ is the final projectile hydrogen-like wavefunction in the 3B case. The 4B case final projectile wavefunction is exactly the same as in the CB1 method, except that in the BCIS-4B case we only considered capture into the final ground state $\varphi_{\rm P}(\vec{s}_1)\equiv\varphi_{100}(\vec{s}_1)$. Functions $N^-(\nu_{\rm T}){}_1F_1(-i\nu_{\rm T},1,-ivx-i\vec{v}\cdot\vec{x})$ and $N^-(\nu'_{\rm T}){}_1F_1(-i\nu'_{\rm T},1,-ivx_1-i\vec{v}\cdot\vec{x}_1)$ are electronic Coulomb waves centered on the target nuclei (screened in the 4B case). They are composed of a confluent hypergeometric function ${}_1F_1(a,b,z)$, and a normalization constant $N^-(\nu'')$. Looking at Eqs. (13) and (14), and comparing Eq. (14) with Eq. (11), we can now infer the essential difference between the CB1 and BCIS methods. Namely, while CB1 methods consider single-electron capture as a direct process, BCIS methods treat it as a two-step mechanism: the electron is first ionized (occupying a continuum intermediate state, given by the electronic Coulomb wave), after which capture occurs from this intermediate ionized state. In this sense, CB1 methods belong to the class of first-order theories, while BCIS methods belong to the class of second-order theories. As previously stated, the main topic of this paper is to study exactly the influence of inclusion of intermediate ionization states upon the values of calculated cross sections.

The transition amplitudes for the prior and post version of the CB1-4B method can now be written as:

$$\begin{aligned}T_{if}^-(\vec{\eta}) &= Z_{\rm P}\int\int\int {\rm d}\vec{R}\,{\rm d}\vec{x}_1\,{\rm d}\vec{x}_2\\ &\quad\times e^{-i\vec{\alpha}\cdot\vec{R}-i\vec{v}\cdot\vec{x}_1}(vR+\vec{v}\cdot\vec{R})^{i\xi}\\ &\quad\times\varphi^*_{nlm}(\vec{s}_1)\varphi^*_{100}(\vec{x}_2)\varphi_i(\vec{x}_1,\vec{x}_2)\\ &\quad\times\left(\frac{2}{R}-\frac{1}{s_1}-\frac{1}{s_2}\right)\,, \qquad (15)\\ T_{if}^+(\vec{\eta}) &= \int\int\int {\rm d}\vec{R}\,{\rm d}\vec{x}_1\,{\rm d}\vec{x}_2\\ &\quad\times e^{-i\vec{\alpha}\cdot\vec{R}-i\vec{v}\cdot\vec{x}_1}(vR+\vec{v}\cdot\vec{R})^{i\xi}\\ &\quad\times\varphi^*_{nlm}(\vec{s}_1)\varphi^*_{100}(\vec{x}_2)\varphi_i(\vec{x}_1,\vec{x}_2)\\ &\quad\times\left[Z_{\rm P}\left(\frac{1}{R}-\frac{1}{s_2}\right)+(Z_{\rm T}-1)\left(\frac{1}{R}-\frac{1}{x_1}\right)\right.\\ &\quad\left.+\left(\frac{1}{r_{12}}-\frac{1}{x_1}\right)\right]\,, \qquad (16)\end{aligned}$$

while the prior versions of the BCIS-3B and BCIS-4B methods are given by the following equations:

$$\begin{aligned}T_{if}^{3B}(\vec{\eta}) &= Z_{\rm P}\int\int {\rm d}\vec{R}\,{\rm d}\vec{s}\\ &\quad\times e^{i\vec{\beta}\cdot\vec{R}-i\vec{v}\cdot\vec{s}}(vR+\vec{v}\cdot\vec{R})^{i\xi}\\ &\quad\times\varphi^*_{nlm}(\vec{s})\varphi_{100}(\vec{x})\\ &\quad\times\left(\frac{1}{R}-\frac{1}{s}\right)N^+(\nu_{\rm T})\\ &\quad\times{}_1F_1(i\nu_{\rm T},1,ivx+i\vec{v}\cdot\vec{x})\,, \qquad (17)\\ T_{if}^{4B}(\vec{\eta}) &= Z_{\rm P}\int\int\int {\rm d}\vec{R}\,{\rm d}\vec{s}_1\,{\rm d}\vec{s}_2\\ &\quad\times e^{i\vec{\beta}\cdot\vec{R}-i\vec{v}\cdot\vec{s}_1}(vR+\vec{v}\cdot\vec{R})^{i\xi}\\ &\quad\times\varphi^*_{100}(\vec{s}_1)\varphi^*_{100}(\vec{x}_2)\varphi_i(\vec{x}_1,\vec{x}_2)\\ &\quad\times\left(\frac{2}{R}-\frac{1}{s_1}-\frac{1}{s_2}\right)N^+(\nu_{\rm T})\\ &\quad\times{}_1F_1(i\nu_T,1,ivx_1+i\vec{v}\cdot\vec{x}_1)\,, \qquad (18)\end{aligned}$$

where $N^+(\nu'') = [N^-(\nu'')]^*$ holds.

Differential and total cross sections are, respectively, given by:

$$\frac{\mathrm{d}Q}{\mathrm{d}\Omega}\left(\frac{a_0^2}{sr}\right) = \frac{\mu^2}{4\pi^2}|T_{if}(\vec{\eta})|^2\,, \tag{19}$$

$$Q(\pi a_0^2) = \frac{1}{2\pi^2 v^2}\int_0^\infty \mathrm{d}\eta\eta|T_{if}(\vec{\eta})|^2\,, \tag{20}$$

where $\eta \approx 2\mu v \sin\frac{\theta}{2}$ is the transversal momentum transfer vector, while $\theta = \arccos(\hat{\vec{k}}_i \cdot \hat{\vec{k}}_f)$ and $\mu = \frac{M_\mathrm{P} M_\mathrm{T}}{M_\mathrm{P}+M_\mathrm{T}}$.

3 Results and discussion

In this section, the results will be presented for both the differential and total, state-resolved and state-summed cross sections. Using the state-resolved cross sections $Q_{nlm}^{\mathrm{tot/dif}}$ for capture into arbitrary nlm states, we can calculate the state-resolved cross sections $Q_{nl}^{\mathrm{tot/dif}}$ and $Q_n^{\mathrm{tot/dif}}$ for capture into resolved nl and n states, respectively, using the following equations:

$$Q_{nl}^{\mathrm{tot/dif}} = \sum_{m=-l}^{l} Q_{nlm}^{\mathrm{tot/dif}}\,, \tag{21}$$

$$Q_n^{\mathrm{tot/dif}} = \sum_{l=0}^{n-1} Q_{nl}^{\mathrm{tot/dif}}\,. \tag{22}$$

As indicated, these equations hold for both the differential and total cross sections. State-summed cross sections are obtained by explicitly including the contributions from all $Q_n^{\mathrm{tot/dif}}$ up to some $n_{\max}$, and approximating the contributions from higher excited states with $n > n_{\max}$ via the Oppenheimer n^{-3} scaling law [1]:

$$Q_\Sigma^{\mathrm{tot/dif}} \simeq \sum_{n=1}^{n_{max}-1} Q_n^{\mathrm{tot/dif}} + \gamma(n_{\max}) Q_{n_{\max}}^{\mathrm{tot/dif}}\,. \tag{23}$$

The first four values of the $\gamma(n_{\max})$ function from Eq. (23) are $\gamma(1) = 1.202$, $\gamma(2) = 1.616$, $\gamma(3) = 2.081$ and $\gamma(4) = 2.561$.

The results of prior form CB1-4B [29], post form CB1-4B [30], as well as prior forms of BCIS-3B [32] and BCIS-4B [33] will be presented. The results will include both differential and total cross sections. For the case of total cross sections, nl state-resolved results with $n \leq 4$ of the prior and post form CB1-4B, as well as the prior form BCIS-3B method will be included. Unfortunately, BCIS-4B results for capture into arbitrary final states are currently unavailable, so no state-resolved BCIS-4B cross sections will be presented. The BCIS-4B results for state-summed cross sections will nevertheless be included, through the use of available final ground-state results, as well as the Oppenheimer scaling law (23) with $n_{\max} = 1$. In the differential cross sections case, since no state-resolved experimental data are available, only state-summed cross sections will be included, for prior and post form CB1-4B, as well as prior form BCIS-4B method. The BCIS-3B differential cross sections are unavailable in the literature.

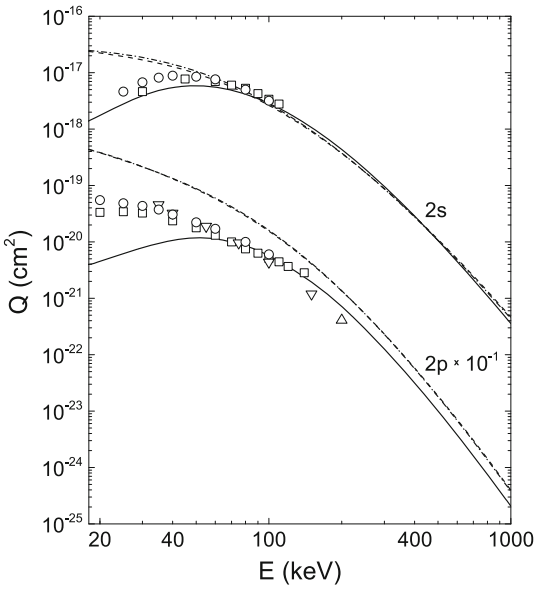

Fig. 1 State-selective total cross sections Q_{2s} and Q_{2p} as a function of impact energy for single-electron capture by protons from He($1s^2$). Theoretical results: dashed line—CB1-4B prior [29], dash-dotted line—CB1-4B post [30], full line—BCIS-3B [32]. Experimental data: □ Hughes et al. [64], ○ Cline et al. [65], △ Hippler et al. [66], ▽ Hippler et al. [67]. Both the theoretical and experimental results for Q_{2p} are divided by 10

We will first present the state-resolved total cross section results for capture into the $2s$, $2p$, $3s$, $3p$, $3d$, $4s$ and $4p$ states, followed by the state-summed total cross sections for capture into all final states. Finally, the state-summed differential cross sections for an intermediate energy of 100 keV, as well as a high energy of 7.5 MeV will be given. All the results are presented in a graphical form, along with comparisons with experimental data wherever they are available.

Regarding the state-resolved total cross sections, Fig. 1 provides Q_{2s} and Q_{2p} cross sections, while Fig. 2 depicts the Q_{3s}, Q_{3p} and Q_{3d} cross sections. Finally, the results for Q_{4s} and Q_{4p} are presented in Fig. 3. All the mentioned state-resolved cross sections come with available sets of measurements for comparison, except the Q_{4p} cross sections.

We will first analyze the situation with spherically-symmetric ($l = 0$) state-resolved cross sections. Looking at Figs. 1, 2, 3, we can immediately notice that the prior and post form CB1-4B methods yield almost indistinguishable results. Therefore, when comparing

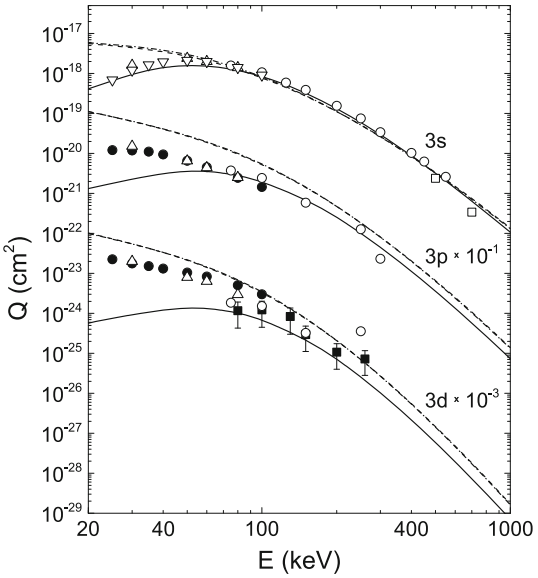

Fig. 2 The same as in Fig. 1, except for state-selective total cross sections Q_{3s}, Q_{3p} and Q_{3d}, and for different sets of measurements. Experimental data: ○ Ford et al. [68], □ Conrads et al. [69], △ Brower and Pipkin [70], ▽ Cline et al. [65], • Cline et al. [71], ■ Edwards and Thomas [72]. Both the theoretical and experimental results are divided by a factor: Q_{3p} by 10 and Q_{3d} by 10^3

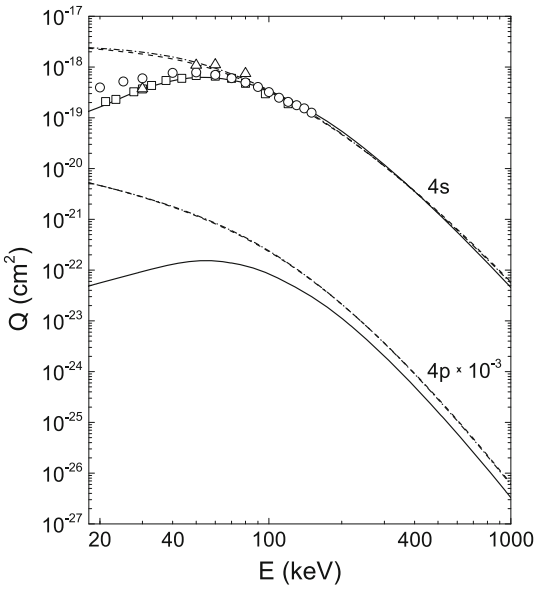

Fig. 3 The same as in Fig. 1, except for state-selective total cross sections Q_{4s} and Q_{4p}, and for different sets of measurements. Experimental data: □ (Q_{4s}) Hughes et al. [73], ○ Doughty et al. [74], △ Brower and Pipkin [70]. The theoretical results for Q_{4p} are divided by 10^3

with BCIS-3B cross sections, we can conclude that all the differences stem from the inclusion of intermediate ionization continua, as well as, of course, the simplifying assumptions underlying the BCIS-3B application to p + He collisions. While all three methods provide practically the same cross section values and in accordance with the experiments above around 70 keV, below this energy the CB1-4B and BCIS-3B methods diverge from one another. This is actually in favor of the BCIS-3B method, since it almost perfectly agrees with the measurements down to the lowest displayed energy values. The CB1-4B methods, on the other hand, overestimate the measurements below 70 keV. We can therefore conclude that the inclusion of continuum intermediate states indeed yields crucial results, as it markedly improves the agreement with measurements, even when using an effective model.

Moving to the spherically-asymmetric states with $l = 1$, Figs. 1 and 2 provide even more useful insights. Namely, the prior and post CB1-4B curves almost completely overlap, and overestimate the Q_{2p} and Q_{3p} measurements in the whole displayed energy interval. The BCIS-3B method, however, almost perfectly agrees with the experiments above around 60 keV. Therefore, the importance of intermediate ionization continua is again evident. Below 60 keV, the BCIS-3B method does underestimate the measurements. This can probably be attributed to the application of the effective three-body method. The fully developed BCIS-4B is expected to correct this discrepancy. Note that a difference was indeed expected at lower energy values, since a slower projectile has more time to interact with the target and "see" its structure. At higher energies, small interaction times essentially "blur" the structure of the target, providing ground for the application of effective three-body methods to four-body problems. As previously seen, this problem was not encountered for $l = 0$ states, at least for $E \geq 20$ keV. Figure 3 shows a completely analogous situation with respect to the different theories, but with no available measurements to make a comparison with.

Finally, Fig. 2 shows the results for Q_{3d}. This is the only example where the effective three-body method fails, and CB1-4B approximations yield better results (and again almost the same for prior and post versions). The BCIS-3B method underestimates measurements in the whole available energy interval, although the BCIS-3B line does begin to approach the experiments around about 80 keV. We have to note that while they do provide better results, CB1-4B methods still overestimate the measurements a bit in the whole energy interval. Again, judging from the previously analyzed situations, the authors hypothesize that the best results would again be provided by a full four-body BCIS theory.

Figure 4 depicts the results of all the four theories, compared with measurements, for state-summed total cross sections. As can be seen from the figure, all four methods provide more-or-less the same cross sections above around 60 keV. There are of course some discrepancies, but not to a large extent. Prior and post CB1-4B forms are almost indistinguishable in the whole interval. The relation between the CB1-4B methods, the BCIS-3B method and the measurements is similar to the one encountered in the case of state-resolved cross sections in the previous figures. Namely, below

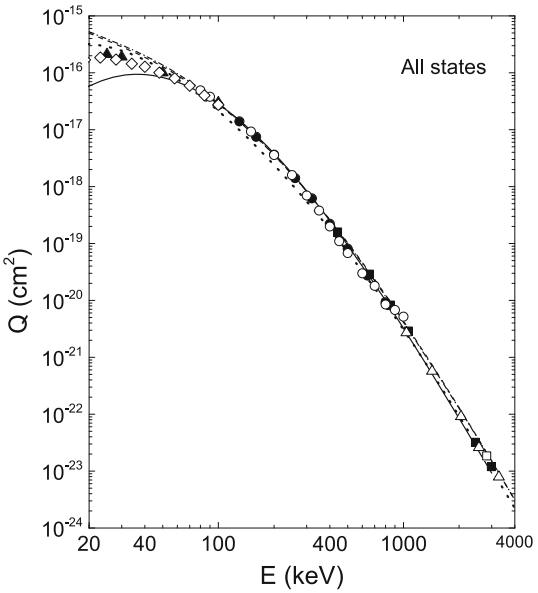

Fig. 4 State-summed total cross sections Q_Σ as a function of impact energies for single-electron capture by protons from He($1s^2$) into all the final bound states H(Σ). Theoretical results: dashed line—CB1-4B prior [29], dash-dotted line—CB1-4B post [30], full line—BCIS-3B [32], dotted line—BCIS-4B [33]. Experimental data: ■ Welsh et al. [75], △ Scryber [76], ○ Williams [77], ▲ Martin et al. [78], □ Horsdal-Pedersen et al. [79], ● Shah and Gilbody [80], ◊ Shah et al. [81]

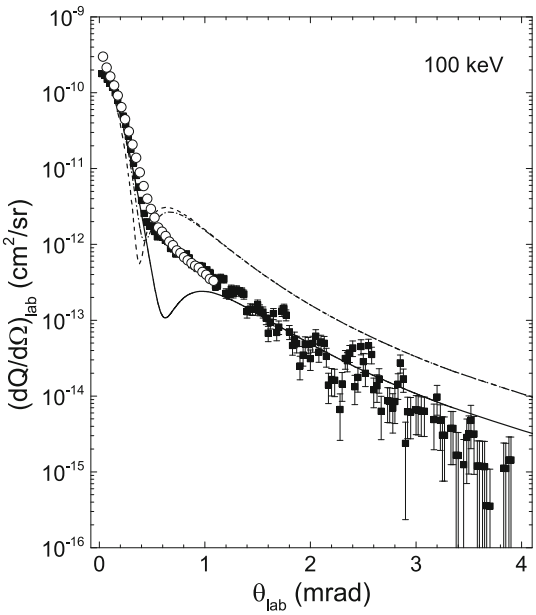

Fig. 5 State-summed differential cross sections $(dQ/d\Omega)_\Sigma$ as a function of scattering angle θ in the laboratory frame of reference for single-electron capture by protons from He($1s^2$) at the intermediate impact energy $E = 100$ keV. Theoretical results: dashed line—CB1-4B prior [29], dash-dotted line—CB1-4B post [30], full line—BCIS-4B [33]. Experimental data: ■ Schöffler et al. [82], ○ Guo et al. [83]

60 keV, CB1-4B methods begin to overestimate, while BCIS-3B begins to underestimate the measurements. The BCIS-4B method, although it also overestimates the measurements below 60 keV a bit, provides cross section values the closest to experimental ones. This again demonstrates the critical importance of the ionization continua, which naturally manifests in the state-summed total cross sections as well. For lower energies, CB1-4B methods fail due to the lack of inclusion of the continuum intermediate states. Since BCIS-3B and BCIS-4B methods provide almost indistinguishable cross section values for sufficiently high energies (above about 700 keV), and both belong to the same class of second-order methods, almost all the differences between them for lower energy values can be attributed to the simplifying assumptions underlying the effective three-body method, when applied to a fundamentally four-body problem. As previously explained, at higher energies, the projectile moves very fast, effectively making the target's structure "obscured." Due to this, the passive electron does not bear much influence on the capture of the active electron, since the projectile does not "see" it that well. At lower energies, the projectile moves significantly slower, thereby unmasking the influence of the passive electron. The difference of almost an order of magnitude in BCIS-3B and BCIS-4B cross sections at 20 keV can be attributed to the unjustified neglect of the passive electron's influence in the three-body formalism, for low energy values. Note that some of the discrepancy could also originate in the use of the non-exact helium ground-state wavefunction in the four-body case.

Now, for a more stringent test of the discussed theoretical approaches, differential cross sections will be considered. An intermediate-energy value of 100 keV, as well as a high-energy value of 7.5 MeV was chosen for comparisons. This enables us to have more inclusive evaluation of the presented methods.

Figure 5 displays the CB1-4B prior and post, as well as the BCIS-4B differential cross sections at $E = 100$ keV. The cross sections are state-summed, and measurements are available for comparison. As can be seen from the figure, prior and post CB1-4B forms cross sections are almost indistinguishable above around 0.80 mrad. The important thing to note is that for angles smaller than this, there is a noticeable difference between the two forms (in contrast with the total cross sections situation). Nevertheless, this difference does not significantly impact the overall picture, at least in terms of agreement with the measurements. Figure 5 undoubtedly demonstrates the contribution of continuum intermediate states with respect to differential cross sections at intermediate impact energy values. While all methods exhibit unphysical minima at certain angles, CB1-4B methods either under or overestimate the measurements in almost the whole displayed energy region. The agreement with experiments is satisfactory only for a narrow forward-scattering region. The BCIS-4B method, on the other hand, excellently reproduces the measurements for almost all angles considered, with

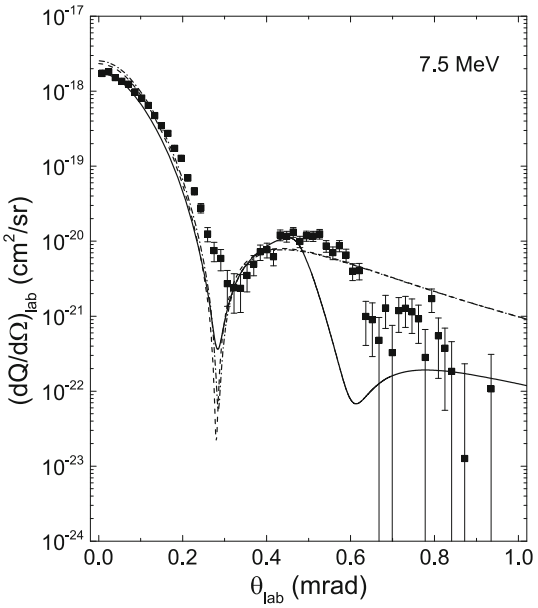

Fig. 6 The same as in Fig. 5, except for the high impact energy $E = 7.5\,\text{MeV}$, and for a different set of measurements. Experimental data: ■ Fischer et al. [85]

the exception of a window around the unphysical minimum, where there exists a significant underestimation. This dip is expected to be at least partially filled with the explicit inclusion of excited states (we remind that they are here only approximately included for all $n > 1$, via (23)).

Finally, Fig. 6 presents the CB1-4B prior and post, and the BCIS-4B prior differential cross section results at $E = 7.5\,\text{MeV}$. In this case, the prior and post CB1-4B forms are almost indistinguishable in the whole energy interval (in contrast with the intermediate-energy case). A bit of a difference again occurs around the dip, but is not as pronounced as in the $E = 100\,\text{keV}$ case. In general, the BCIS-4B method again provides a better agreement with the experiments than CB1-4B ones. All methods work extremely well for forward scattering. Both the CB1-4B and BCIS-4B methods exhibit a dip at about the same angle of 0.28 mrad, which is more pronounced in the CB1-4B, than in the BCIS-4B case. However, in contrast with the intermediate energy case (Fig. 5), the dip here is indeed observed in the measurements, as can be seen in Fig. 6. It can although be noted that the dip's position in the measurements is slightly shifted toward larger scattering angles, and the dip itself is not as pronounced as in the theoretical methods' results. Perhaps the most important result seen in Fig. 6 is that the BCIS-4B method perfectly predicts Thomas double-scattering, i.e., the second peak at about $\theta = 47\,\text{mrad}$. This is a quantum mechanical analogue of the classical Thomas billiard-type double collision, in which the electron is captured by first colliding with the projectile, then the target, then proceeding to move almost in parallel with the projectile. In the classical picture, capture occurs due to this parallel movement of the projectile and electron. All second-order theories (which the BCIS-4B method belongs to) predict this experimentally detected Thomas double-scattering peak, and this is a clear advantage of second-order methods. The CB1-4B, being first-order methods, are unable to predict this peak, as demonstrated in Fig. 6. Further away from the Thomas peak (i.e., at larger angles), the CB1-4B and BCIS-4B methods provide drastically different results ($1 - 2$ orders of magnitude different values). Due to large experimental errors in this region, it is difficult to truly assess which method is superior here, although the measurements do seem to favor BCIS-4B. Moreover, the BCIS-4B method predicts a second dip after the Thomas peak, which also seems to be confirmed by the measurements. While the dip is again not as pronounced in the measurements, its position seems to coincide with the theoretically predicted one. Note that, due to large experimental errors for angles larger than the ones corresponding to the Thomas peak, it is difficult to draw any conclusions with absolute certainty. Another noteworthy observation is the second peak predicted by the BCIS-4B method, which also seems to be corroborated by the measurements. The origin of this peak is due to Rutherford scattering, which becomes the dominant scattering mechanism for larger angle values.

4 Conclusion

The main goal of this work was to investigate the impact of continuum intermediate states upon the cross section values for single-electron capture in collisions of fast protons with ground-state helium atoms. Through the inclusion of these intermediate states, single-electron capture can be interpreted as a two-step mechanism, where the electron first becomes ionized (thus occupying the continuum intermediate state), with capture taking place from this ionized intermediate state. The investigation of influence of these states was conducted by comparing the results of two theories which include them: the BCIS-3B and BCIS-4B methods, with the results of two theories which do not include continuum intermediate states: the CB1-4B prior and post form methods. The comparisons were performed for state-resolved and state-summed total cross sections, as well as state-summed differential cross sections, at both intermediate and high impact energies. For all the considered scenarios, barring few exceptions, the BCIS methods consistently performed better with respect to measurements. This was particularly true at lower energies for total cross sections, as well as the whole angular interval for differential cross sections at the intermediate impact energy $E = 100\,\text{keV}$. Also, regarding differential cross sections at a high impact energy of $E = 7.5\,\text{MeV}$, we have seen that the Thomas double-scattering peak can be successfully reproduced only with a second-order theory (such as the BCIS-4B), while first-order theories (such as CB1-4B) fail in this regard. Taking all of the above into account, we reach the conclusion that continuum intermediate

states are indeed extremely important for the most accurate reproduction of the experiments, for both total and differential cross sections. Particular importance of the continuum intermediate states is noted at lower and intermediate energies, as well as for some high-energy features (Thomas double scattering) in the differential cross sections.

Regarding the possible future lanes of work, the most straightforward and productive would obviously be the extension of BCIS-4B method to explicitly consider capture into arbitrary excited states. This could definitely clear up the situation with state-resolved cross sections, as well as offer some further improvements with the state-summed cross sections. As previously discussed, full BCIS-4B results would be expected to produce the best alignment with the measurements.

As previously stated in Introduction, aside from the fundamental considerations, the present study regarding single-electron capture is important due to various interdisciplinary applications, such as astrophysics [49], thermonuclear fusion and plasma physics [50–53], and medical physics [8,54–61].

Acknowledgements The author thanks the Ministry of Education, Science and Technological Development of the Republic of Serbia for support under Contract No. 451-03-68/2022-14/200124. The material presented and discussed in this paper is based on the author's oral progress report, given at the 31st Summer School and International Symposium on the Physics of Ionized Gases (Belgrade, Serbia, September 5–9, 2022). The abstract of this progress report was previously published in the symposium's *Book of contributed papers & abstracts of invited lectures, topical invited lectures and progress reports* [39].

Data Availability Statement This manuscript has no associated data or the data will not be deposited. [Authors' comment: The datasets (cross section data) generated and/or analyzed during the current study are available from the corresponding author upon reasonable request].

Declarations

Conflict of interest The author declares that he has no known competing funding, employment, financial or non-financial interests that could have appeared to influence the work reported in this paper.

References

1. J.R. Oppenheimer, Phys. Rev. **31**, 349 (1928)
2. H.C. Brinkman, H.A. Kramers, Proc. Acad. Sci. Amst. **33**, 973 (1930)
3. Dž. Belkić, Principles of Quantum Scattering Theory, Institute of Physics, Bristol (2004)
4. I.M. Cheshire, Proc. Phys. Soc. Lond. **84**, 89 (1964)
5. Dž. Belkić, R. Gayet, A. Salin, Phys. Rep. **56**, 279 (1979)
6. Dž. Belkić, *Quantum Theory of High-Energy Ion-Atom Collisions* (Taylor and Francis, Oxford, 2008)
7. Dž. Belkić, I. Mančev, J. Hanssen, Rev. Mod. Phys. **80**, 249 (2008)
8. Dž. Belkić (ed.), *Theory of Heavy Ion Collisions in Hadron Therapy*, vol. 65 (Elsevier, Amsterdam, 2013)
9. E. Ghanbari-Adivi, A.N. Velayati, Cent. Eur. J. Phys. **11**, 423 (2013)
10. S.K. Datta, D.S.F. Crothers, R. McCarroll, J. Phys. B **23**, 479 (1990)
11. S.K. Datta, J. Phys. B **25**, 1001 (1990)
12. I. Mančev, N. Milojević, Dž. Belkić, At. Data Nucl. Data Tables **129–130**, 101282 (2019)
13. T. Kirchner, H.J. Lüdde, R.M. Dreizler, Phys. Rev. A **61**, 012705 (1999)
14. T. Kirchner, M. Horbatsch, M. Keim, H.J. Lüdde, Phys. Rev. A **69**, 012708 (1999)
15. A.E. Martinez, G.R. Deco, R.D. Rivarola, P.D. Fainstein, Nucl. Inst. Meth. Phys. Res. B **34**, 32 (1988)
16. P.N. Abufager, A.E. Martinez, R.D. Rivarola, P.D. Fainstein, Nucl. Inst. Meth. Phys. Res. B **233**, 255 (2005)
17. M.S. Gravielle, J.E. Miraglia, Phys. Rev. A **38**, 5034 (1988)
18. T.G. Winter, Phys. Rev. A **47**, 264 (1993)
19. T.G. Winter, Phys. Rev. A **48**, 3706 (1993)
20. S. Houamer, Yu.V. Popov, C. Dal Cappello, Phys. Lett. A **373**, 4447 (2009)
21. D.S.F. Crothers, K.M. Dunseath, J. Phys. B **20**, 4115 (1987)
22. H. Marxer, J.S. Briggs, J. Phys. B **25**, 3823 (1992)
23. I. Mančev, N. Milojević, Dž. Belkić, Eur. Phys. J. D **72**, 209 (2018)
24. E. Ghanbari-Adivi, H. Ghavaminia, Int. J. Mod. Phys. E **24**, 1550093 (2015)
25. E. Ghanbari-Adivi, J. Phys. B **44**, 165204 (2011)
26. I. Mančev, N. Milojević, Dž. Belkić, EPL **103**, 23001 (2013)
27. I. Mančev, N. Milojević, Dž. Belkić, At. Data Nucl. Data Tables **102**, 6 (2015)
28. N. Milojević, I. Mančev, Dž. Belkić, Phys. Rev. A **96**(3), 032709 (2017)
29. I. Mančev, N. Milojević, Dž, Belkić. Phys. Rev. A **86**, 022704 (2012)
30. I. Mančev, N. Milojević, Dž, Belkić. Phys. Rev. A **88**, 052706 (2013)
31. N. Milojević, J. Phys. Conf. Ser. **565**, 012004 (2014)
32. N. Milojević, I. Mančev, D. Delibašić, Dž. Belkić, Phys. Rev. A **102**, 012816 (2020)
33. I. Mančev, N. Milojević, Dž. Belkić, Phys. Rev. A **91**, 062705 (2015)
34. I. Mančev, N. Milojević, D. Delibašić, Dž. Belkić, Phys. Scr. **95**(6), 065403 (2020)
35. D. Delibašić, N. Milojević, I. Mančev, Dž. Belkić, At. Data Nucl. Data Tables **139**, 101417 (2021)
36. D. Delibašić, N. Milojević, I. Mančev, Dž. Belkić, Eur. Phys. J. D **75**, 115 (2021)
37. D. Delibašić, N. Milojević, I. Mančev, Dž. Belkić, At. Data Nucl. Data Tables **148**, 101530 (2022)
38. D. Delibašić, N. Milojević, I. Mančev, F.U. Phys, Chem. Tech. **18**(2), 131 (2020)
39. D. Delibašić, Publ. Astron. Obs. Belgrade **102**, 29 (2022)

40. R. Shakeshaft, Phys. Rev. A **18**, 1930 (1978)
41. X.M. Tong, D. Kato, T. Watanabe, S. Ohtani, Phys. Rev. **62**, 052701 (2000)
42. S.K. Avazbaev, A.S. Kadyrov, I.B. Abdurakhmanov, D.V. Fursa, I. Bray, Phys. Rev. A **93**, 022710 (2016)
43. I.B. Abdurakhmanov, J.J. Bailey, A.S. Kadyrov, I. Bray, Phys. Rev. A **97**, 032707 (2018)
44. M. Zapukhlyak, T. Kirchner, Phys. Rev. A **80**, 062705 (2009)
45. M. Baxter, T. Kirchner, Phys. Rev. A **93**, 012502 (2016)
46. A. Igarashi, C.D. Lin, Phys. Rev. Lett. **83**, 4041 (1999)
47. I.B. Abdurakhmanov, A.S. Kadyrov, S.K. Avazbaev, I. Bray, J. Phys. B **49**, 115203 (2016)
48. J. Faulkner, I.B. Abdurakhmanov, S.U. Alladustov, A.S. Kadyrov, I. Bray, Plasma Phys. Control. Fusion **61**, 095005 (2019)
49. T.E. Cravens, Science **296**, 1042 (2002)
50. R.C. Isler, Plasma Phys. Control. Fusion **6**, 171 (1994)
51. D.M. Thomas, Phys. Plasmas **19**, 056118 (2012)
52. R. Hemsworth, H. Decamps, J. Graceffa, B. Schunke, M. Tanaka, M. Dremel, A. Tanga, H.P.L. De Esch, F. Geli, J. Milnes, T. Inoue, D. Marcuzzi, P. Sonato, P. Zaccaria, Nucl. Fusion **49**, 045006 (2009)
53. H. Anderson, M.G. von Hellermann, R. Hoekstra, L.D. Horton, A.C. Howman, R.W.T. Konig, R. Martin, R.E. Olson, H.P. Summers, Plasma Phys. Control. Fusion **42**, 781 (2000)
54. Dž. Belkić, Z. Med, Phys. **31**, 122 (2021)
55. L.F. Errea, C. Illescas, P.M.M. Gabás, L. Méndez, I. Rabadán, A. Riera, B. Pons, *Fast Ion-Atom and Ion-Molecule Collisions*, ed. by Dž. Belkić, (World Scientific Publishing, Singapore, 2013) p. 231
56. R. Garcia-Molina, I. Abril, P. de Vera, *Fast Ion-Atom and Ion-Molecule Collisions*, ed. by Dž. Belkić, (World Scientific Publishing, Singapore, 2013) p. 271
57. M.A. Rodríguez-Bernal, J.A. Liendo, *Theory of Heavy Ion Collision Physics in Hadron Therapy*, ed. by Dž. Belkić, (Elsevier, Amsterdam, 2013) p. 203
58. R.D. Rivarola, M.E. Galassi, P.D. Fainstein, C. Champion, *Theory of Heavy Ion Collision Physics in Hadron Therapy*, ed. by Dž. Belkić, (Elsevier, Amsterdam, 2013) p. 231
59. C. Champion, J. Hanssen, R.D. Rivarola, *Theory of Heavy Ion Collision Physics in Hadron Therapy*, ed. by Dž. Belkić, (Elsevier, Amsterdam, 2013) p. 269
60. J.J. Bailey, I.B. Abdurakhmanov, A.S. Kadyrov, I. Bray, *State-of-the-Art-Reviews on Energetic Ion-Atom and Ion-Molecule Collisions*, ed. by Dž. Belkić, I. Bray, A. Kadyrov, (World Scientific Publishing, Singapore, 2019) p. 227
61. S. Guatelli, D. Bolst, Z. Francis, S. Inserti, V. Ivanchenko, A.B. Rosenfeld, *State-of-the-Art-Reviews on Energetic Ion-Atom and Ion-Molecule Collisions*, ed. by Dž. Belkić, I. Bray, A. Kadyrov, (World Scientific Publishing, Singapore, 2019) p. 255
62. J.N. Silverman, O. Platas, F.A. Matsen, J. Chem. Phys. **32**, 1402 (1960)
63. P. Löwdin, Phys. Rev. **90**, 120 (1953)
64. R.H. Hughes, E.D. Stokes, C. Song-Sik, T.J. King, Phys. Rev. **4**, 1453 (1971)
65. R. Cline, P.J.M. van der Burgt, W.B. Westerveld, J.S. Risley, Phys. Rev. A **49**, 2613 (1994)
66. R. Hippler, W. Harbich, M. Faust, H.O. Lutz, L.J. Dube, J. Phys. B **19**, 1507 (1986)
67. R. Hippler, W. Harbich, H. Madeheim, H. Kleinpoppen, H.O. Lutz, Phys. Rev. A **35**, 3139 (1987)
68. J.C. Ford, E.W. Thomas, Phys. Rev. A **5**, 1694 (1972)
69. R.J. Conrads, T.W. Nichols, J.C. Ford, E.W. Thomas, Phys. Rev. A **7**, 1928 (1973)
70. M.C. Brower, F.M. Pipkin, Phys. Rev. A **39**, 3323 (1989)
71. R.A. Cline, W.B. Westerveld, J.S. Risley, Phys. Rev. A **43**, 1611 (1991)
72. J.L. Edwards, E.W. Thomas, Phys. Rev. A **2**, 2346 (1970)
73. R.H. Hughes, H.R. Dawson, B.M. Doughty, Phys. Rev. **164**, 166 (1967)
74. B.M. Doughty, M.L. Goad, R.W. Cernosek, Phys. Rev. A **18**, 29 (1978)
75. L.M. Welsh, K.H. Berkner, S.N. Kaplan, R.V. Pyle, Phys. Rev. **158**, 85 (1967)
76. U. Schryber, Helv. Phys. Acta **40**, 1023 (1967)
77. J.F. Williams, Phys. Rev. **157**, 97 (1967)
78. P.J. Martin, K. Arnett, D.M. Blankenship, T.J. Kvale, J.L. Peacher, E. Redd, V.C. Sutcliffe, J.T. Park, C.D. Lin, J.H. McGuire, Phys. Rev. A **23**, 2858 (1981)
79. E. Horsdal-Pedersen, C. Cocke, M. Stockli, Phys. Rev. Lett. **50**, 1910 (1983)
80. M.B. Shah, H.B. Gilbody, J. Phys. B **18**, 899 (1985)
81. M.B. Shah, P. McCallion, H.B. Gilbody, J. Phys. B **22**, 3037 (1989)
82. M.S. Schöffler, J. Titze, L.Ph.H. Schmidt, T. Jehnke, N. Neumann, O. Jagutzki, H. Schmidt-Böcking, R. Dörner, I. Mančev, Phys. Rev. A **79**, 064701 (2009)
83. D.L. Guo, X. Ma, S.F. Zhang, X.L. Zhu, W.T. Feng, R.T. Zhang, B. Li, H.P. Liu, S.C. Yan, P.J. Zhang, Q. Wang, Phys. Rev. A **86**, 052707 (2012)
84. P. Loftager, Private communication (2002)
85. D. Fischer, M. Gudmundsson, Z. Berényi, N. Haag, H.A.B. Johansson, D. Misra, P. Reinhed, A. Källberg, A. Simonsson, K. Stöchkel, H. Cederquist, H.T. Schmidt, Phys. Rev. A **81**, 012714 (2010)